

# Effectiveness of Fiber Lines With Symmetric Dispersion Swing for 160-Gb/s Terrestrial Transmission Systems

J. Fatome, S. Pitois, P. Tchofo Dinda, G. Millot, E. Le Rouzic, B. Cuenot, E. Pincemin, and S. Gosselin

**Abstract**—We demonstrate theoretically and experimentally that a fiber line with a symmetric dispersion swing can substantially improve the performance of 160-Gb/s optical transmissions. The improvement lies in an increased transmission distance and reduction of the optimum input signal power by one order of magnitude compared with that of a conventional system.

**Index Terms**—Dispersion management (DM), optical fiber communication, recirculating loop, ultrashort pulses.

## I. INTRODUCTION

IT IS widely perceived that an appropriate management of the fiber chromatic dispersion is essential for both the designing of the next generation of transmission systems, and the upgrading of the already installed fiber-optic networks to higher time-division-multiplexed bit rates [1]–[5]. Various techniques of dispersion management have been proposed with a view to achieve ultrahigh-speed transmissions (at bit rate more than 40 Gb/s per channel). Hence, for terrestrial transmissions, one commonly makes use of conventional dispersion-managed (DM) systems, in which the map length is equal to (or more than) the amplifier span [4], [6]. In this letter, we demonstrate theoretically and experimentally that the performance of conventional DM systems, which are fundamentally built up from an asymmetric dispersion profile [6], can be substantially improved by using a symmetric profile of dispersion swing.

## II. THEORY

Pulse dynamics in a periodically amplified DM fiber system can be described by the following nonlinear Schrödinger equation (NLSE):

$$u_z + i[\beta_2(z)/2]u_{tt} - ia(z)\gamma(z)|u|^2u = 0 \quad (1)$$

where  $u$  is the normalized envelope of the axial electrical field  $\psi(z, t) = \sqrt{a(z)}u(z, t)$ . The function  $a(z)$  describes energy variations induced by losses and periodic amplification,  $\beta_2$  and

$\gamma$  represent the group velocity dispersion and self-phase modulation parameters, respectively. The usual dispersion parameter  $D$  is given by  $\beta_2 = -\lambda^2 D/(2\pi c)$ , where  $\lambda = 1.55 \mu\text{m}$  is the transmission wavelength. The pulse energy along the line is given by  $E = a(z)E_0$ , where  $E_0 = \int_{-\infty}^{+\infty} |u|^2 dt$  is a constant of motion of (1). Using a Gaussian ansatz, one can express the NLSE (1) in terms of a set of ordinary differential equations for the dynamics of the pulse parameters [7]

$$\dot{\xi} = [4Ca\gamma E_0 \xi] / [\sqrt{\pi}x_3^3] \quad (2a)$$

$$\dot{C} = \beta_2 + [2a\gamma E_0(C^2 - 1/\xi^2)] / [\sqrt{\pi}x_3^3]. \quad (2b)$$

In (2), the over-head dot represents the derivative with respect to  $z$ . The square root of  $\xi \equiv 2(1 + b^2)/x_3^2$ , with  $b \equiv -x_4 x_3^2/2$ , is proportional to the spectral bandwidth of the pulse, and  $C \equiv b/\xi$  is the cumulated dispersion. The parameter  $x_4/(2\pi)$  represents the pulse chirp. The specific features of the transmission systems under consideration come from the asymmetric and symmetric nature of their dispersion maps, as can be seen in Fig. 1(a1) and (a2), respectively. The asymmetric map (AM) is the standard map for the existing terrestrial transmission systems. This map consists of two sections of fibers: a single-mode fiber (SMF) with the following typical parameters, dispersion  $D^- = 17 \text{ ps/nm/km}$ , dispersion slope  $S^- = 0.06 \text{ ps/nm}^2/\text{km}$ , length  $L^- = 100 \text{ km}$ , losses  $\alpha^- = 0.2 \text{ dB/km}$ , effective core area  $A_{\text{eff}}^- = 80 \mu\text{m}^2$ , followed by a dispersion compensating fiber (DCF), with typical parameters  $D^+ = -90 \text{ ps/nm/km}$ ,  $L^+ = |D^- L^- / D^+|$ ,  $S^+ = -(S^- L^- / L^+)$ ,  $\alpha^+ = 0.6 \text{ dB/km}$ , and  $A_{\text{eff}}^+ = 20 \mu\text{m}^2$ . In the present study, we employ a double-stage amplification [6], in three distinct cases. The first case corresponds to the classical situation, where the gain  $G_1$  of the first amplifier (placed just before the DCF) is tuned so as to compensate for the total (distributed or lumped) losses over the first section of the map, while the second amplifier with gain  $G_2$  compensates for the total losses over the second section of the map. This case (where  $G_2 \neq G_1$ ) corresponds to the classical asymmetric map (CAM) [4]. The second configuration corresponds to a “modified asymmetric map” (MAM) with  $G_2 = G_1$ . For the third configuration, we use a symmetric map (SM) that consists of three sections of fibers ( $L_-/2, L_+, L_-/2$ ), as Fig. 1(a2) shows, and two amplifiers with equal gains. We have not considered elements of precompensation and postcompensation of dispersion in any of the three systems. The length of the period of dispersion swing is  $Z_D = L^+ + L^- = 120 \text{ km}$ . Each period is repeated to build up the line associated with each configuration.

Manuscript received December 4, 2003; revised June 9, 2004. This work was supported by a contract between the University of Burgundy and the France Telecom R&D (Contract 42 56 26 63). The work of J. Fatome was supported by the Conseil Regional de Bourgogne and the Centre National de la Recherche Scientifique.

J. Fatome, S. Pitois, P. Tchofo Dinda, and G. Millot are with the Laboratoire de Physique, Université de Bourgogne, Unité Mixte de Recherche, CNRS, 21078 Dijon Cédex, France (e-mail: spitois@u-bourgogne.fr).

E. Le Rouzic, B. Cuenot, E. Pincemin, and S. Gosselin are with France Telecom R&D RTA/OCN/TALE 2, 22300 Lannion, France.

Digital Object Identifier 10.1109/LPT.2004.834587

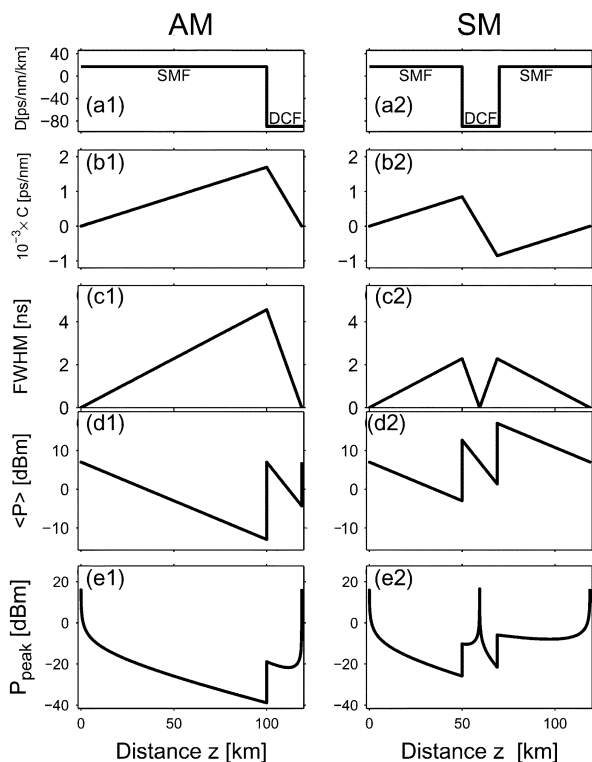


Fig. 1. Variational analysis. (a1), (a2) Dispersion map. (b1), (b2) Cumulated dispersion  $C$ . (c1), (c2) Pulsewidth. (d1), (d2) Means power  $\langle P \rangle$ . (e1), (e2) Peak power  $P_{\text{peak}}$ .

Using the variational equations (2), we have obtained the evolution of the pulse parameters within one dispersion map, for an input chirp-free Gaussian pulse with the following typical parameters: full-width at half-maximum (FWHM) 1.3 ps and peak power  $P_{\text{peak}} = 45$  mW. The results are given in Fig. 1, which exhibit the following features: The fast dynamics of the CAM and MAM exhibit essentially the same general features, except very slight differences in the evolution of the peak power and mean power. But fundamental differences between the AM and the SM are clearly visible in Fig. 1. Indeed, the AM leads to a maximum pulse broadening that is almost two times larger than in the case of the SM [see Fig. 1(c1) and (c2)]. Hence, the pulsewidth in the AM grows up to  $\sim 4650$  ps, thus implying that if a pulse train is launched in the line, then each pulse will interact with its neighbors over a total range of  $\sim 730$  bit slots, whereas in the SM the interaction range is reduced to  $\sim 320$  bit slots. Here lies a crucial qualitative difference that makes the SM more advantageous, and that will make transmission of pulse trains in the AM more prone to pulse interactions and related effects such as generation of ghost pulses and amplitude fluctuation by intrachannel four-wave mixing [3]. The second major difference between the two systems appears in Fig. 1(d1) and (d2), which shows that the mean power  $\langle P \rangle$  in the AM decreases to a minimum value (at the end of the SMF), which is one order of magnitude lower than the minimum value of the mean power in the SM. This implies that if the same input power is used for both the SM and the AM, the signal-to-noise ratio (SNR) will experience very severe degradations in the AM. But this drawback of the AM can be resolved by using a sufficiently large input power. The third important feature lies in the evolution of

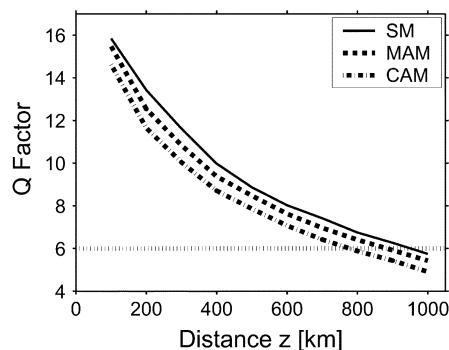


Fig. 2.  $Q$  factor obtained from numerical simulations of the NLSE.

the peak power. Fig. 1(e1) and (e2) shows that in the AM, the peak power attains its maximum value at the junction point between the end of DCF and the beginning of the SMF, whereas, in the SM, the peak power attains its maximum value at the middle of the DCF. Consequently, the high nonlinearity of DCF will make the SM more prone to nonlinear effects than the AM can be. But this drawback of the SM can be resolved by using a sufficiently low input power. It comes out from this analysis that, if a careful optimization of the input power is carried out for each configuration, then it may be possible to obtain equivalent levels of SNR and nonlinear effects in the two systems, but such an optimization procedure cannot resolve the drawback of the AM related to its long range of pulse interactions.

We have also illustrated the effectiveness of the SM through numerical simulations of transmission of 1024-bit pseudo-random binary sequence patterns of Gaussian pulses in a single channel lines operating at 160 Gb/s, with an amplifier noise figure of 5 dB, Gaussian filters with bandwidth 1.8 THz. For the simulations, we have solved the generalized NLSE including the third-order dispersion and amplifier noise, by means of a split-step Fourier simulation tool [8]. In these simulations, we have not included the stimulated Raman scattering and polarization-mode dispersion (PMD). The transmission performance is evaluated by means of the  $Q$  factor in linear units.  $Q = 6$  corresponds to a bit-error ratio (BER) of  $10^{-9}$ . We defined the *transmission distance*  $L_{\text{max}}$  as the distance over which the  $Q$  factor remains higher than six. Fig. 2 shows the results that we have obtained by carefully optimizing the input peak power ( $P_{\text{opt}}$ ) for each system to achieve maximum transmission distance ( $L_{\text{max}}$ ). We then find the following transmission performances: CAM:  $P_{\text{peak}} = 23$  mW and  $L_{\text{max}} = 700$  km; MAM:  $P_{\text{peak}} = 35$  mW and  $L_{\text{max}} = 800$  km; SM:  $P_{\text{peak}} = 3$  mW and  $L_{\text{max}} = 900$  km. It comes out that the MAM leads to a slightly better transmission distance than that of the CAM, but at the expense of an increased optimum power (by  $\sim 50\%$ ). But here, the most interesting feature lies in the optimum power required for the SM ( $P_{\text{peak}} = 3$  mW), which is reduced by one order of magnitude compared with the optimum power for the AMs. This power reduction is achieved without any sacrifice on the transmission distance, and even with a slight increase of the transmission distance by  $\sim 10\%$  compared with the case of the AM. Thus, the possibility to use substantially low pulse powers in the SM is interesting for reducing the power budget in wavelength-division-multiplexing (WDM) transmissions.

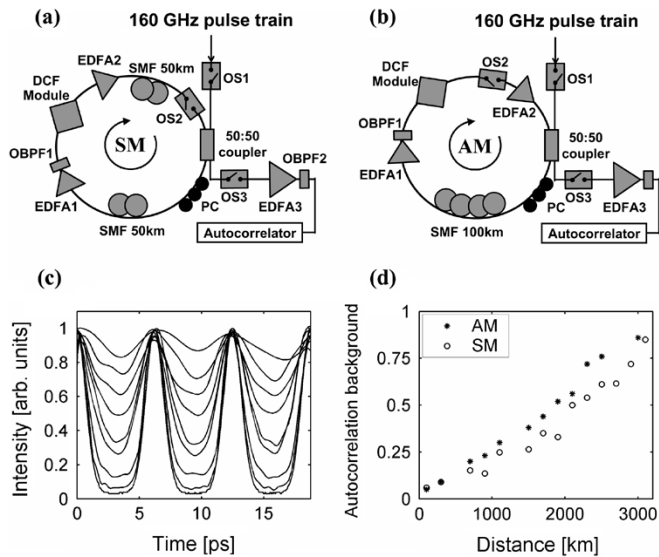


Fig. 3. Experimental setup for the (a) SM and (b) AM. (c) Evolution of the autocorrelation trace of the 160-GHz pulse train as a function of propagation distance for the SM. (d) Evolution of the autocorrelation function background of the 160-GHz pulse train as a function of propagation distance in the AM loop (stars) and SM loop (circles).

### III. EXPERIMENT

To experimentally examine the transmission performance of the lines described above, we have built up two different recirculating loops corresponding to the SM and AM, as can be seen in Fig. 3(a) and (b), respectively. Using four-wave mixing and nonlinear reshaping processes [9], 160-GHz transform-limited pedestal-free Gaussian pulses with 1.27 ps of FWHM were generated and injected in each loop. The average PMD of each loop was measured and found to be around  $0.07 \text{ ps/km}^{1/2}$ . As we do not study PMD effects in this letter, a polarization controller was used inside the loop to minimize degradations due to PMD, thus simulating the effect of a PMD compensator. Two lumped amplifiers with noise figure of 5.5 dB [erbium-doped fiber amplifier (EDFA 1 and EDFA 2)] were inserted in each loop to compensate for the fiber and coupling losses (44.2 dB). A Gaussian filter [optical bandpass filter (OBPF1)] of bandwidth 1.8 THz was used to reduce the amplified spontaneous emission noise. The quality of the transmission was evaluated by means of the autocorrelation trace of the pulse train [10]. The autocorrelation technique is helpful to carry out comparisons between the transmission performances of different systems, when classical BER testing equipments are not available [11]. Fig. 3(c) illustrates the evolution of the autocorrelation trace of the pulse train, as a function of the propagation distance for the SM (from bottom to top at  $z = 0, 100, 900, 1500, 1900, 2100, 2700, 2900$  and  $z = 3100 \text{ km}$ ). We observe that signal degradations progressively and inevitably take place as the propagation distance increases, but with a signal profile that can still be clearly observed and analyzed up to  $\sim 3000 \text{ km}$  (30 round-trips). On the other hand, Fig. 3(d), which represents the evolution of the autocorrelation trace background as a function of the propagation distance for both the SM and the AM, shows that at any distance the SM leads to a clearly better quality of transmission. Quantitatively, for the same background, the SM leads to a propagation

distance that is  $\sim 20\%$  (in average) larger than that of the AM. More importantly, the average input power measured just after the 50 : 50 coupler was found to be 9 dBm for the AM and only  $-1 \text{ dBm}$  for the SM, thus confirming that the SM requires an optimum input power that is one order of magnitude less than that of the AM. Thus, the experimental results confirm the theoretical prediction of the superior performances of the SM over the AM for 160-Gb/s transmissions.

### IV. CONCLUSION

In this letter, we have demonstrated that a fiber line in which the period of the dispersion swing consists of three alternating sections of SMF and DCF ( $L_-/2, L_+, L_-/2$ ), can substantially improve the performance of high-speed terrestrial systems. Much of the improvement lies in an increased transmission distance, and an optimum input power which is one order of magnitude less than that required for a conventional system [6].

Finally, a useful extension of the present work will be to examine the performance of those systems in WDM transmissions. Without being too speculative, we suspect that the SM, which requires a strongly reduced energy without any sacrifice on the transmission distance, may reduce the impact of detrimental nonlinear effects such as stimulated Raman scattering or cross-phase modulation, resulting from collisions of pulses of different channels of a WDM system.

### REFERENCES

- [1] D. Breuer, F. Küppers, A. Mattheus, E. G. Shapiro, I. Gabitov, and S. K. Turitsyn, "Symmetrical dispersion compensation for standard monomode-fiber-bases communication systems with large amplifier spacing," *Opt. Lett.*, vol. 22, pp. 982–984, 1997.
- [2] D. Breuer, K. Jürgensen, F. Küppers, A. Mattheus, I. Gabitov, and S. K. Turitsyn, "Optical schemes for dispersion compensation of standard monomode fiber bases links," *Opt. Commun.*, vol. 140, pp. 15–18, 1997.
- [3] P. V. Mamyshev and N. A. Mamysheva, "Pulse-overlapped dispersion-managed data transmission and intrachannel four-wave mixing," *Opt. Lett.*, vol. 24, pp. 1454–1457, 1999.
- [4] M. Nakazawa, H. Kubota, K. Suzuki, E. Yamada, and A. Sahara, "Ultrahigh-speed long-distance TDM and WDM soliton transmission technologies," *IEEE J. Select. Topics Quantum Electron.*, vol. 6, pp. 363–396, Mar./Apr. 2000.
- [5] L. J. Richardson, W. Forsysiak, and N. J. Doran, "Trans-oceanic 160-GBIT/s single-channel transmission using short-period dispersion management," *IEEE Photon. Technol. Lett.*, vol. 13, pp. 209–211, Mar. 2001.
- [6] B. Cuenot, "Comparison of engineering scenarios for  $N \times 160 \text{ Gb/s}$  WDM transmission systems," *IEEE Photon. Technol. Lett.*, vol. 15, pp. 864–866, June 2003.
- [7] V. E. Zakharov and S. Wabnitz, *Optical Solitons: Theoretical Challenges and Industrial Perspectives*, Berlin, Germany: Springer-Verlag, 1998.
- [8] "VPI Transmission Maker," VPIsystems Inc, Berlin, Germany, 1998.
- [9] S. Pitois, J. Fatome, and G. Millot, "Generation of a 160-GHz transform-limited pedestal-free pulse train through multiwave mixing compression of a dual-frequency beat signal," *Opt. Lett.*, vol. 27, pp. 1729–1731, 2002.
- [10] J. Fatome, S. Pitois, P. Tchofo Dinda, and G. Millot, "Experimental demonstration of 160-GHz densely dispersion-managed soliton transmission in a single channel over 896 km of commercial fibers," *Opt. Express*, vol. 11, pp. 1553–1558, 2003.
- [11] A. Maruta, Y. Yamamoto, S. Okamoto, S. Suzuki, T. Morita, A. Agata, and A. Hasegawa, "Effectiveness of densely dispersion-managed soliton in ultra-high transmission," *Electron. Lett.*, vol. 36, pp. 1947–1949, 2000.